

## **STRUCTURAL ANALYSES, MICROSTRUCTURAL CHARACTERISTICS AND ELECTRICAL CONDUCTIVITY OF COPPER-COBALT FERRITES**

Khin Sandar Soe<sup>1</sup>, Nyo Nyo Myint<sup>2</sup>, Thida Nyunt Than<sup>3</sup> & Win Kyaw<sup>3</sup>

### **Abstract**

Solid electrolyte materials of Copper-Cobalt ferrites with the general formula,  $\text{Cu}_{1-x}\text{Co}_x\text{Fe}_2\text{O}_4$  (where  $x = 0.00, 0.33$  and  $1.00$ ), were prepared by chemical co-precipitation method. Structural analyses of the samples were investigated by X-ray diffraction (XRD) method. XRD patterns revealed that the samples analogous to cubic structure and the lattice parameters were found to be increased with increase in concentration of Co. The crystallite sizes were obtained in the range of 29.85 nm – 43.44 nm. Scanning Electron Microscopy was used to study the microstructural properties of the sample. SEM micrographs showed that the grain shapes and sizes were affected by the concentration of Co and the most intergranular porosities were found in Cu-Co ferrite of  $x = 0.33$  sample among the investigated materials. The electrical conductivities of the samples were investigated in the temperature range of 303 K – 873 K to study the superionic conductivities and to evaluate the activation energies of the samples for the applications of solid electrolyte materials.

**Keywords:** Copper-Cobalt ferrites, chemical co-precipitation method, XRD, SEM, superionic conductivities

### **Introduction**

Ferrites are electrically ferrimagnetic ceramic compound materials, consisting of various mixtures of iron oxides such as Hematite ( $\text{Fe}_2\text{O}_3$ ) or Magnetite ( $\text{Fe}_3\text{O}_4$ ) and oxides of other metals like NiO, CuO, ZnO, MnO, CoO [Fang, (2003); Kumar, (2009)]. The prime property of ferrites is that, in the magnetized state, all spin magnetic moments are not oriented in the same direction. Few of them are in the opposite direction. But as the spin magnetic moments are of two types with different values, the net magnetic moment will have some finite value [Harris, (2009); Rani, (2013)].

<sup>1</sup> Dr, Demonstrator, Department of Physics, Monywa University

<sup>2</sup> Dr, Associate Professor, Department of Physics, Yenanchaung Degree College

<sup>3</sup> Dr, Associate Professors, Department of Physics, Sagaing University

Copper ferrite is one of the important spinel ferrites  $MFe_2O_4$  because it exhibits phase transitions, changes semiconducting properties, shows electrical switching and tetragonality variation when treated under different conditions in addition to interesting magnetic and electrical properties with chemical and thermal stabilities [Kumar, (2009); Shutka, (2010)]. It is used in wide range of applications in gas sensing, catalytic applications, Li ion batteries high density magneto-optic recording devices, color imaging, bioprocessing, magnetic refrigeration and Ferro fluids [Tailhades, (1998)]. In this work,  $Cu_{1-x}Co_xFe_2O_4$  (where  $x = 0.00, 0.33$  and  $1.00$ ) were prepared by using chemical co-precipitation method and their structural, microstructural and electrical characteristics were studied by XRD, SEM and temperature dependent electrical resistance measurements for the application of solid electrolyte materials.

## **Materials and Method**

### **Preparation of Copper-Cobalt Ferrite**

$Cu_{1-x}Co_xFe_2O_4$  (where  $x = 0.00, 0.33$  and  $1.00$ ) were prepared by chemical co-precipitation method from Oxalate precursors. Raw materials of Analytical Reagent (AR) grade Cupric Chloride ( $CuCl_2 \cdot 2H_2O$ ), Cobalt Chloride ( $CoCl_2 \cdot 6H_2O$ ), and Ferric Chloride Hexahydrate ( $FeCl_3 \cdot 6H_2O$ ) with stoichiometric composition were used to prepare the sample.

In the first, a concentrated solution of Cupric, Cobaltous, and Ferric Chlorides were reacted with an Oxalic acid solution to get a precipitate of Oxalates. The metallic salts were initially dissolved in a mixture of water ( $H_2O$ ), Ethylene Glycol ( $C_2H_6O_6$ ), and Hydrochloric acid ( $HCl$ ), while the Oxalic acid ( $H_2C_2O_4 \cdot 2H_2O$ ) were also dissolved in the mixture of (95%) Ethyl Alcohol ( $C_2H_7OH$ ) and (5%) water. Then, the precursor co-precipitated Cu-Co ferrites were slowly decomposed at  $700^\circ C$  for 5 h in vacuum chamber. Finally, the candidate material of Copper-Cobalt ferrite was obtained.

The flow-diagram of the  $Cu_{1-x}Co_xFe_2O_4$  preparation procedure is shown in Figure 1. Photographs of the starting materials, solutions of starting materials, mixed solution of starting materials, precursor solution and as-prepared Copper-Cobalt ferrite, DELTA A Series Temperature Controller DTA4896 and experimental setup of sample preparation system are shown in Figure 2(a – g).

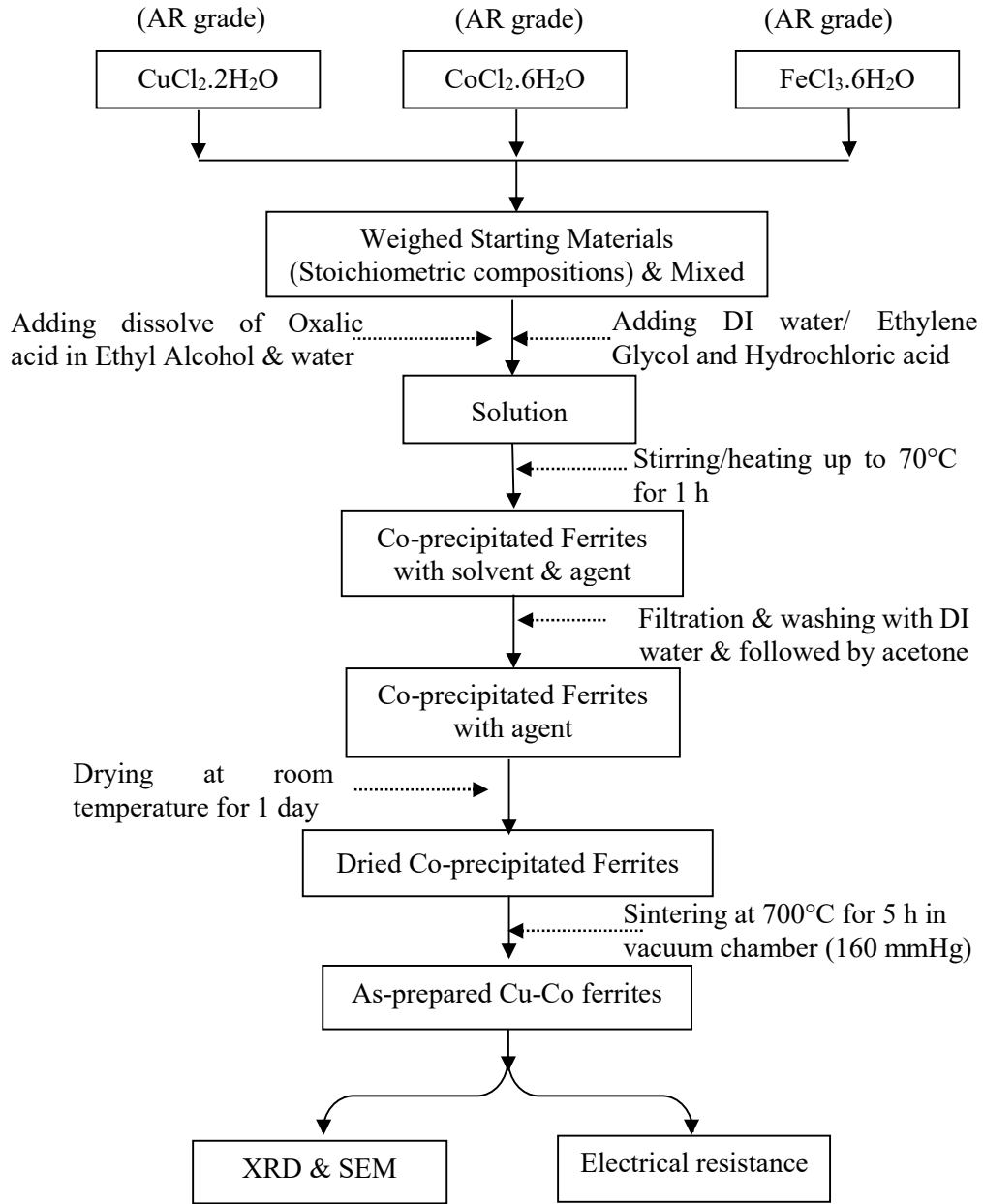


**Figure 1.** Flow-diagram of Cu-Co ferrite preparation

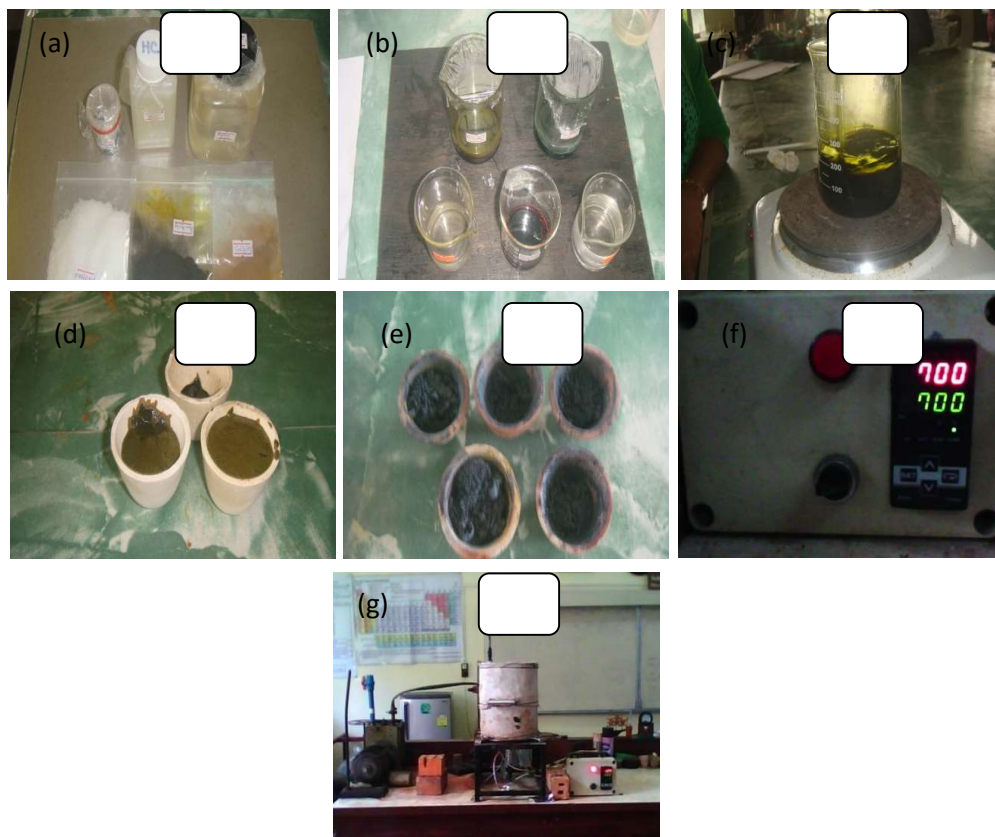
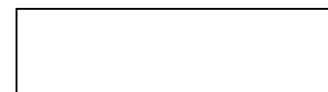
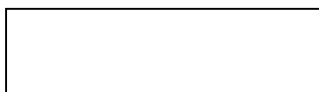


**Figure 1.** Photographs of the (a) starting materials, (b) solutions of starting materials, (c) mixed solution of starting materials, (d) precursor solution, (e) as-prepared Copper-Cobalt ferrite, (f) DELTA A Series Temperature Controller DTA4896 and (g) experimental setup of sample preparation system

### **Characteristic Measurement**

The XRD spectra of the samples were observed by RIGAKU MULTIFLEX X-Ray Diffractometer to analyse the structural characteristics. Morphological features were investigated by using JEOL JSM-5610LV SEM with the accelerating voltage of 15 kV, the beam current of 50 mA and 5500 times of photo magnification. For the temperature dependent electrical resistance measurement, the as-prepared samples were made into pellets. The



silver paste (conductive pen) was made over the sample to ensure good electrical contacts. The electrical resistances of the samples were observed by using FLUKE 45 Dual-display digital multi-meter in the temperature range of 302 K – 873 K. Photograph of the experimental setup of electrical resistance measurement is shown in Figure 3. The area of pellets are  $1.14 \times 10^{-4} \text{ m}^2$  and the thicknesses of the samples are 3.88 mm.



**Figure 3.** Photograph of the experimental setup of temperature dependent electrical resistance measurement

## **Results and Discussion**

### **X-Ray Diffraction Analysis**

Powder X-ray diffraction patterns of the samples are shown in Figure 4(a – c). The observed XRD lines were identified by using standard JCPDS data library files of

- (i) Cat. No.77-0010 >  $\text{CuFe}_2\text{O}_4$  – Copper Iron Oxide for  $x = 0.00$  sample of pure Cu ferrite,
- (ii) Cat. No.22-1086 >  $\text{CoFe}_2\text{O}_4$  – Cobalt Iron Oxide and Cat. No. 77-0010 >  $\text{CuFe}_2\text{O}_4$  – Copper Iron Oxide for  $x = 0.33$  sample of Cu-Co ferrite and
- (iii) Cat. No. 22-1086 >  $\text{CoFe}_2\text{O}_4$  – Cobalt Iron Oxide for  $x = 1.00$  sample of pure Co ferrite

XRD patterns show the formation of single phase cubic structure with only one dominant peak corresponding to (311) reflection indicating that the crystallites are preferentially oriented along (311) plane. In the collected XRD patterns, only one diffraction line of (311) plane is found to be identified because the peak heights of the patterns are very low, i.e., peak heights of other lines are less than 10. Thus it cannot be assigned with JCPDS. The lattice parameters are evaluated by using crystal utility of the equation of

$$\frac{\sin^2 \theta}{(h^2 + k^2 + l^2)} = \frac{\lambda^2}{4a^2}$$

where  $\theta$  is the diffraction angle ( $^\circ$ ), (hkl) is the miller indices,  $\lambda$  is the wavelength of incident X-ray ( $\text{\AA}$ ) and  $a$  is the lattice parameter of the samples ( $\text{\AA}$ ). The observed and evaluated lattice parameters and the unit cell volume of the samples are tabulated in Table 1. Figure 5 shows the variation of the lattice parameters and the unit cell volumes with increase in Co concentration of  $\text{Cu}_{1-x}\text{Co}_x\text{Fe}_2\text{O}_4$  ferrites. The lattice parameter of the  $\text{CuFe}_2\text{O}_4$  was found to be increased with increase in Co concentration. The increase in lattice constant and unit cell volume is due to the smaller ionic radii of the doped cation, i.e.,  $\text{Co}^{2+}$  (0.745  $\text{\AA}$ ) than that of  $\text{Cu}^{2+}$  (0.730  $\text{\AA}$ ). The crystallite sizes of the samples were estimated by using the Scherrer formula,

$$D = \frac{0.9\lambda}{B \cos \theta}$$

where  $D$  is the crystallite size (nm),  $\lambda$  is the wavelength of incident X-ray ( $\text{\AA}$ ),  $\theta$  is the diffraction angle of the peak under consideration at FWHM ( $^\circ$ ) and  $B$  is the observed FWHM (radians). To examine the nanosized ferrite materials, the FWHM of the strongest peak ( $I = 100\%$ ) of (311) planes of the XRD patterns were used to calculate the crystallite size. The obtained crystallite sizes of  $\text{Cu}_{1-x}\text{Co}_x\text{Fe}_2\text{O}_4$  samples are presented in Table 1. It indicates that the as-prepared Cu-Co ferrites powders are nanosized materials and these Cu-Co ferrites are very fine particles nature.

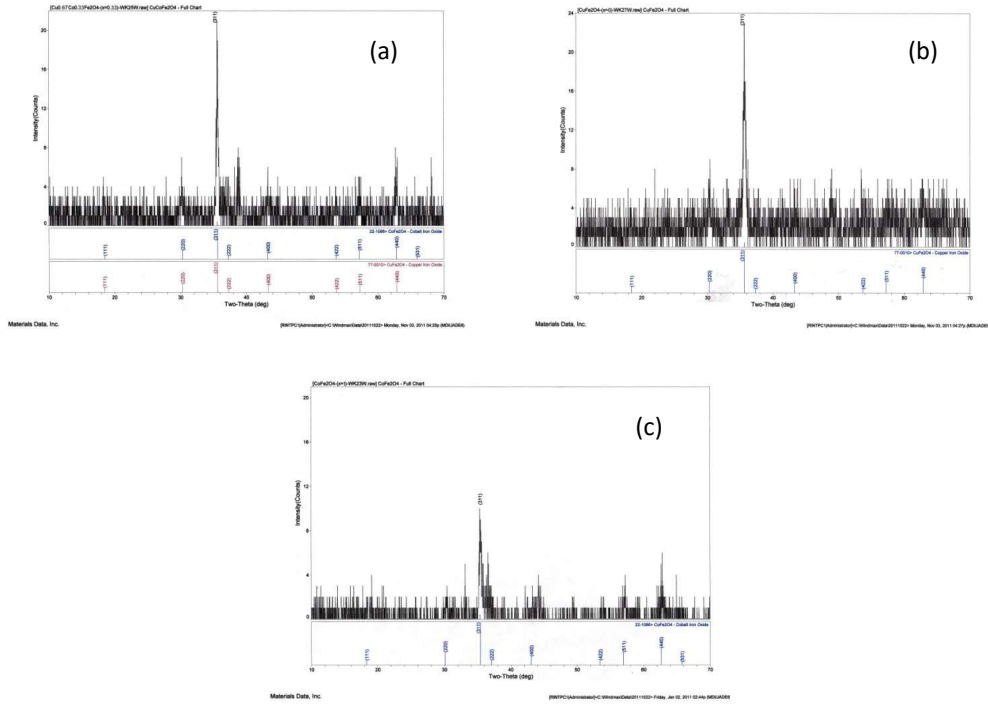


**Figure 4.** XRD patterns of  $\text{Cu}_{1-x}\text{Co}_x\text{Fe}_2\text{O}_4$  for (a)  $x = 0.00$ , (b)  $x = 0.33$  and (c)  $x = 1.00$

**Table 1.** The lattice parameters and crystallite sizes of  $\text{Cu}_{1-x}\text{Co}_x\text{Fe}_2\text{O}_4$

$x$	FWHM ( $^\circ$ )	Obs. $a=b=c$ ( $\text{Å}$ )	Cal. $a=b=c$ ( $\text{Å}$ )	$V$ ( $\text{Å}^3$ )	$D$ (nm)
0.00	0.266	8.347	8.347	581.618	29.85
0.33	0.192	8.360	8.360	584.277	43.44
1.00	0.217	8.406	8.407	594.081	38.42

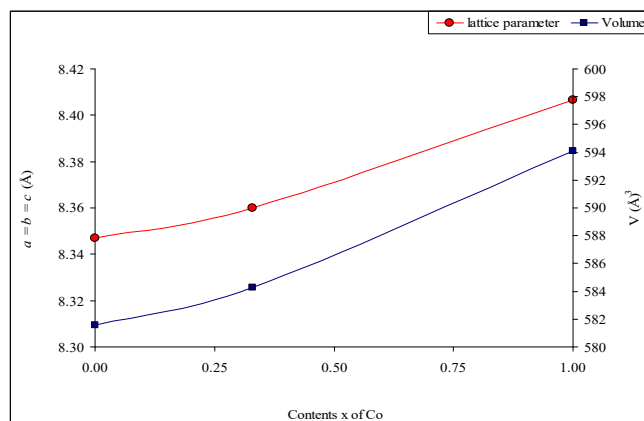


**Figure 5.** Variations of the lattice parameters and the unit cell volumes with increase in concentration of Co of the  $\text{Cu}_{1-x}\text{Co}_x\text{Fe}_2\text{O}_4$  ( $x = 0.00, 0.33$  and  $1.00$ ) samples

### Microstructural Analysis

As more and more attentions have been devoted to the sub-micro magnetic materials for their unique properties compared to their bulk counterparts, the scientific interest on copper-cobalt ferrite is on the rising. SEM micrographs of the  $\text{Cu}_{1-x}\text{Co}_x\text{Fe}_2\text{O}_4$  ( $x = 0.00, 0.33$  and  $1.00$ ) samples are shown in Figure 6(a – c).

In Figure 6(a), the grain shape of the sample is non-uniform rod shape with clear grain boundary. The grain sizes of the sample are in the range of  $0.40 \mu\text{m} - 2.00 \mu\text{m}$ . As shown in SEM micrograph of Cu-Co ferrite, the grain shape of the sample is non-uniform rectangular shape. The grain sizes of the sample are in the range of  $1.00 \mu\text{m} - 8.50 \mu\text{m}$ . In Figure 6(a) and (b), some pores are found due to the decomposition of starting materials.

In Figure 6(c), the grain shape of the sample is spherical shape and the grain sizes are in the range of  $0.20 \mu\text{m} - 0.75 \mu\text{m}$ . Most of samples are found to homogeneous and poor grain boundary. SEM micrographs show that the grain shape of the samples depends on the addition of Co (or composition of desired materials).

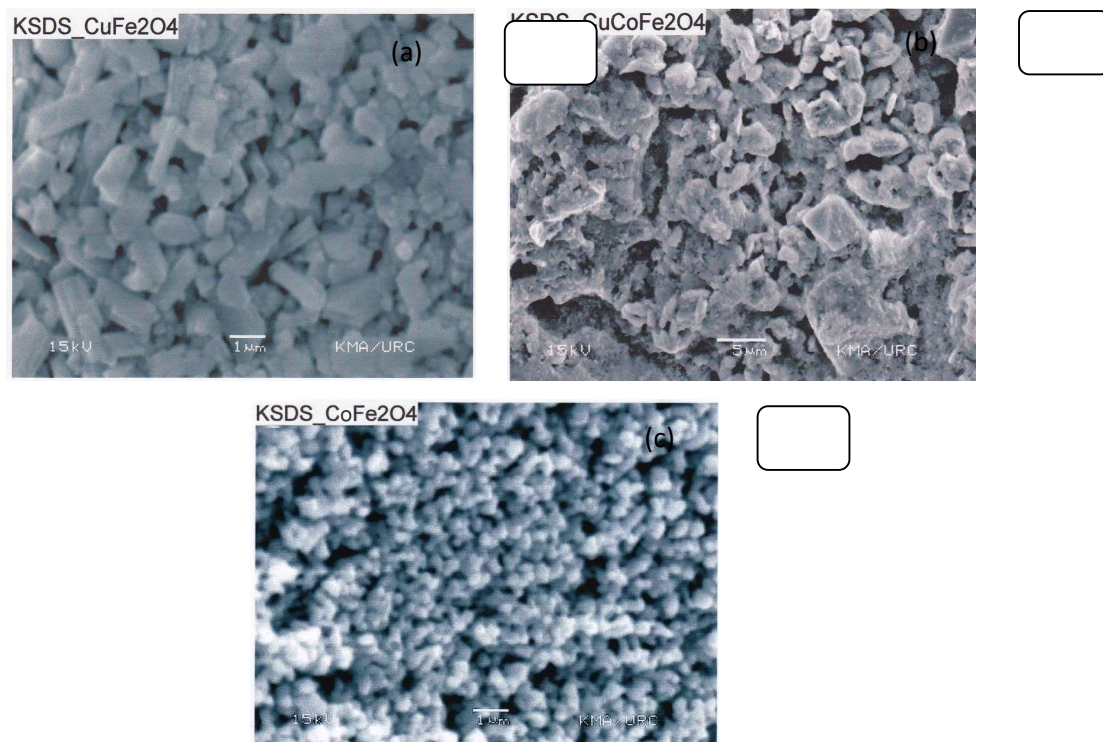


**Figure 5.** SEM micrographs of  $\text{Cu}_{1-x}\text{Co}_x\text{Fe}_2\text{O}_4$  for (a)  $x = 0.00$ , (b)  $x = 0.33$  and (c)  $x = 1.00$

### Temperature Dependent Electrical Conductivity Study

The research in the field of Solid-State Ionic encompasses investigations of the physical and chemical behavior of the solids with fast ion movement within the bulk as well as the technological aspects. These materials widely refer to as “Superionic Solids” or “Solid Electrolytes” or “Fast Ion Conductors”, show tremendous scope to develop all solid-state mini/micro electrochemical devices viz. batteries, fuel cells, sensors, photoelectrochemical solar cells (PECSC) etc. For all-solid-state electrochemical device applications, these solids should have following characteristic properties:

- Ionic conductivity should be high ( $\sim 10^{-1} - 10^{-4} \text{ S cm}^{-1}$ ) and the electronic conductivity should be negligibly small ( $< 10^{-8} \text{ S cm}^{-1}$ ).
- Activation energy should be low ( $< 1 \text{ eV}$ ).

- Ions should be the principal charge carriers and ionic transference number should be close to unity (i.e.  $t_{\text{ion}} \sim 1$ ). They should be a single ion (preferable cation) conducting solids.

The temperature dependent electrical conductivity  $\sigma$  of the ferrites obeys an Arrhenius's expression,  $\sigma = \sigma_0 \exp\left(\frac{-E_a}{kT}\right)$ , where,  $\sigma_0$  is the pre-exponential factor,  $E_a$  is activation energy,  $k$  is Boltzmann's constant and  $T$  absolute temperature. Arrhenius's plots of the dc conductivity with reciprocal temperature of the samples are shown in Figure 7(a – c) in which the temperatures of superionic phase of the samples are indicated with coloured cycles. The graph shows that the increase in temperature leads to increase in conductivity, which is the normal behaviour of superionic materials and it obeys the well known Arrhenius relation. The higher values of temperature for the samples help the trapped charges to be librated and participate in the conduction process which results increase in conductivity. According to the conduction mechanism in ferrites, the decrease in resistivity could also be related to the increase in the drift mobility of the thermally

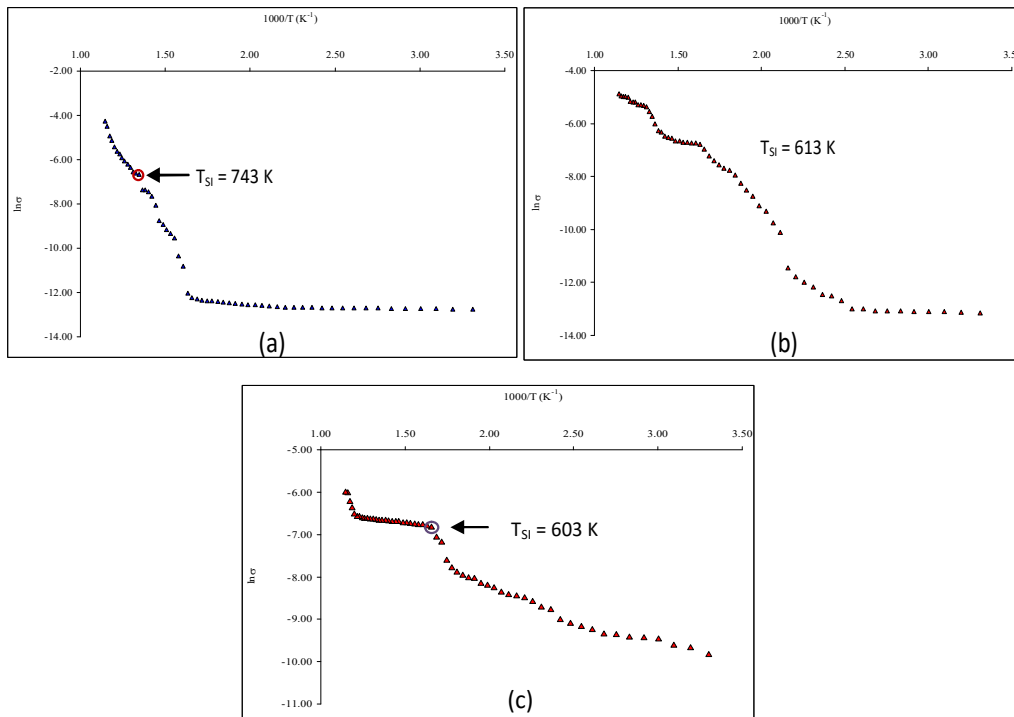


**Figure 7.** Arrhenius plots of the temperature dependent electrical conductivity of  $\text{Cu}_{1-x}\text{Co}_x\text{Fe}_2\text{O}_4$  for (a)  $x = 0.00$ , (b)  $x = 0.33$  and (c)  $x = 1.00$

The electrical conductivity curves can be seen with two portions (temperature regions):

- (i) 303 K – 603 K and (ii) 603 K – 873 K for  $\text{CuFe}_2\text{O}_4$  ( $x = 0.00$ ),
- (i) 303 K – 393 K and (ii) 393 K – 873 K for  $\text{Cu}_{0.67}\text{Co}_{0.33}\text{Fe}_2\text{O}_4$  ( $x = 0.33$ ) and
- (i) 303 K – 603 K and (ii) 603 – 873 K for  $\text{CoFe}_2\text{O}_4$  ( $x = 1.00$ )

to evaluate the activation energies of the samples. Plots of the variations of electrical conductivity of each of the portion of the samples are shown in Figure 8(a) and (b) for  $\text{CuFe}_2\text{O}_4$ , Figure 9(a) and (b) for  $\text{Cu}_{0.67}\text{Co}_{0.33}\text{Fe}_2\text{O}_4$  and Figure 10(a) and (b) for  $\text{CoFe}_2\text{O}_4$  respectively. According to the theory of ionic conductivity, the slope of the electrical conductivity in each of the curves corresponding to the activation energy for creating of defect states due to the ionic motions of the sample due to thermal agitation. The activation energies are obtained as:

- (i) 0.02 eV in 303 K – 603 K and 1.20 eV in 603 K – 873 K for  $\text{CuFe}_2\text{O}_4$ ,
- (ii) 0.0163 eV in 303 K – 393 K and 0.5200 eV in 393 K – 873 K for  $\text{Cu}_{0.67}\text{Co}_{0.33}\text{Fe}_2\text{O}_4$  and
- (iii) 0.1344 eV in 303 K – 393 K and 0.0425 eV in 603 K – 873 K for  $\text{CoFe}_2\text{O}_4$ .

The activation energies are listed in Table 2.

Temperature dependent electrical conductivities of the samples are shown in Figure 11(a – c). The electrical conductivity increases with increase in temperature.

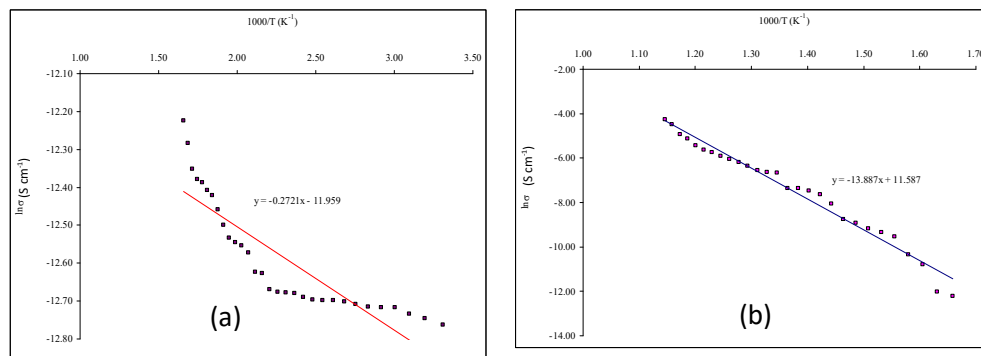


**Figure 8.** Plots of the variations of electrical conductivity of  $\text{Cu}_{1-x}\text{Co}_x\text{Fe}_2\text{O}_4$  for  $x = 0.00$  (a) in 303 K – 603 K and (b) 603 K – 873 K

The samples are exhibited as superionic conductors at high temperatures (743 K – 873 K) for  $\text{CuFe}_2\text{O}_4$ , (613 K – 873 K) for  $\text{Cu}_{0.67}\text{Co}_{0.33}\text{Fe}_2\text{O}_4$  and (603 K – 873 K) for  $\text{CoFe}_2\text{O}_4$  due to their electrical conductivities are found to be  $\sigma > 1 \times 10^{-3} \text{ S m}^{-1}$  in each of the temperature range. It can be said that a few solids conduct electricity better by ion motion than by electron motion. These unusual materials are technologically important in making batteries. All batteries have two electrodes separated by an electrolyte, which is a material that conducts ions better than electrons. Furthermore, the superionic phase temperature decreased with increase in concentration of Co on  $\text{CuFe}_2\text{O}_4$ .

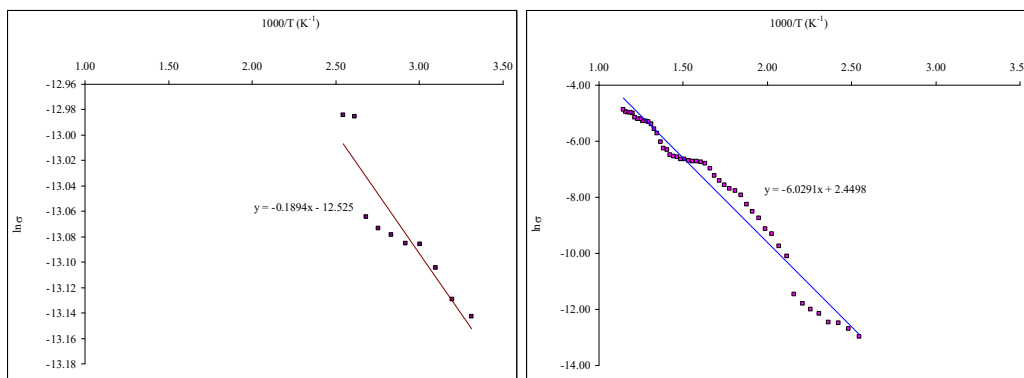


**Figure 9.** Plots of the variations of electrical conductivity of  $\text{Cu}_{1-x}\text{Co}_x\text{Fe}_2\text{O}_4$  for  $x = 0.33$  (a) in 303 K – 393 K and (b) 393 K – 873 K

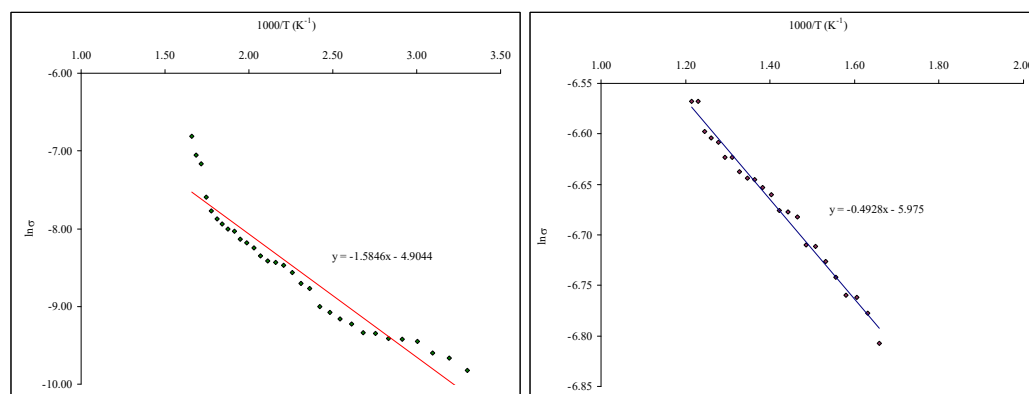


**Figure 10.** Plots of the variations of electrical conductivity of  $\text{Cu}_{1-x}\text{Co}_x\text{Fe}_2\text{O}_4$  for  $x = 1.00$  (a) in 303 K – 603 K and (b) 603 K – 873 K

**Table 2.** The activation energies of  $\text{Cu}_{1-x}\text{Co}_x\text{Fe}_2\text{O}_4$

x	Temperature range (K)	$E_a$ (eV)
0.00	303 - 603	0.02
	603 - 873	1.20
0.33	303 - 393	0.02
	393 - 873	0.52
1.00	303 - 603	0.13
	603 - 873	0.04

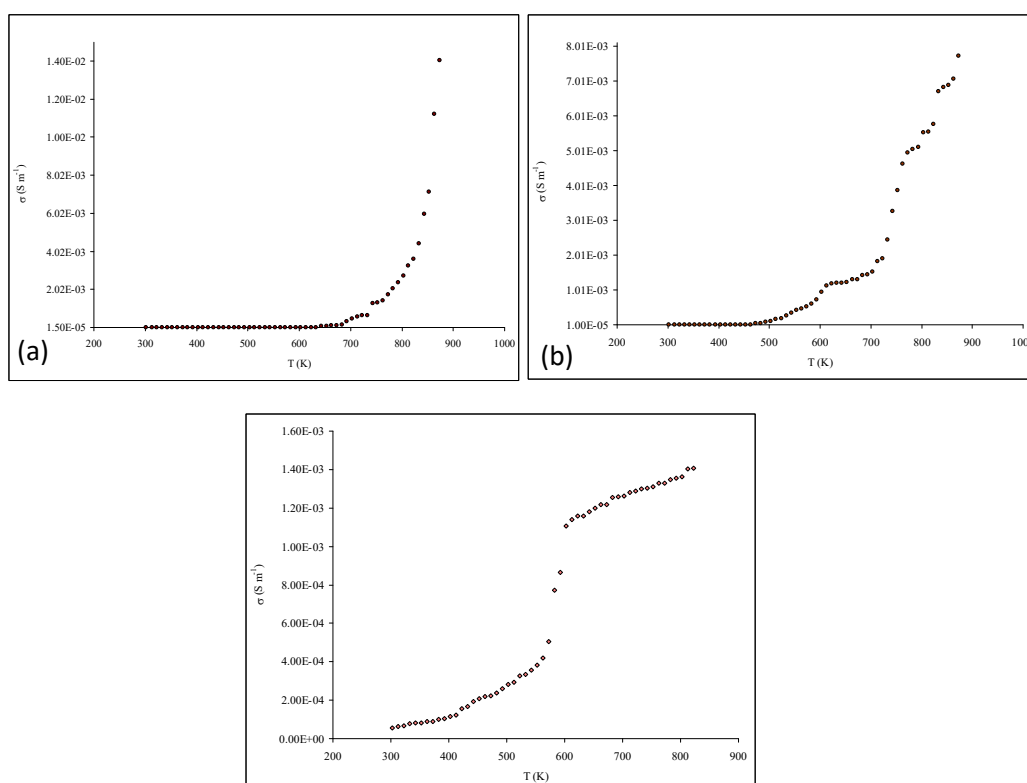


**Figure 11.** Plots of the variation of electrical conductivity with temperature of  $\text{Cu}_{1-x}\text{Co}_x\text{Fe}_2\text{O}_4$  for (a)  $x = 0.00$ , (b)  $x = 0.33$  and (c)  $x = 1.00$

### **Conclusion**

$\text{Cu}_{1-x}\text{Co}_x\text{Fe}_2\text{O}_4$  (where  $x = 0.00, 0.33$  and  $1.00$ ) were prepared by chemical co-precipitation method and their structural, microstructural and electrical conductivities were reported in this work. XRD patterns reveal that the investigated samples analogous to cubic structure. The obtained crystallite sizes indicated that the samples were nanosized materials and very fine particles. SEM micrographs represented three different grain shapes of non-uniform rod for pure Cu ferrite, non-uniform rectangular for Cu-Co ferrite and spherical for pure Co ferrite. Some pores were found in the SEM micrographs due to the decomposition of starting materials in the sample preparation process. The electrical conductivities of the samples were found to be increased with increase in temperature. The samples exhibited as the superionic conductors in the high temperature. The superionic phase temperatures ( $T_{\text{SI}}$ ) of the samples were found to be decreased with increased in Co concentration and found at 743 K for pure Cu ferrite, 613 K for Cu-Co ferrite and 603 K for pure Co ferrite. Except the second portion of the temperature range of pure Cu ferrite, the activation energy of others portions and temperature ranges of the samples were obtained as lower than 1 eV. According to experimental results, the samples can be used as the solid electrolyte materials. Furthermore, from the experimental point of view, pure  $\text{CoFe}_2\text{O}_4$  is the most suitable for the application of solid electrolyte material because it has the lowest superionic conductor phase temperature.

### **Acknowledgement**

The authors would like to acknowledge Professor Dr Khin Khin Win, Head of Department of Physics, University of Yangon, for her kind permission to carry out this work.

## References

1. Fang, J., Sharma, M. & Tang, J. (2003). Ultrafine NiFe<sub>2</sub>O<sub>4</sub> powder fabricated from reverse microemulsion process. *Journal of Applied Physics*, 93(10), pp. 7843-7845.
2. Harris, V.G., He, P., Parimi, P.V., Zuo, X., Patton, C.E., Abe, M., Cher, O. & Vittoria, C. (2009). Recent advances in processing and applications of microwave ferrites. *Journal of Magnetization and Magnetic Materials*, 321, pp. 2035-2047.
3. Kumar, N., Kumar, V., Arora, M., Sharmar, M., Singh, B. & Pant, R.P. (2009). Synthesis of Mn<sub>0.2</sub>Zn<sub>0.8</sub>Fe<sub>2</sub>O<sub>4</sub> particles by high energy ball milling and their applications. *Indian Journal of Engineering and Materials Science*, 16, pp. 410-414.
4. Rani, R., Batoo, K.M. & Singh, M. (2013). Electric and Dielectric Study of Zinc Substituted Cobalt Nanoferrites Prepared by Solution Combustion Method. *American Journal of Nanomaterials*, 1, pp. 9-12.
5. Shutka, A., Mezinskis, G. & Pludon, A. (2010). Preparation of dissimilarly structured ferrite compounds by sol-gel auto-combustion method. *Chemical Technology*, 1(54), pp. 41-46.
6. Tailhades, Ph., Villette, C., & Rousset, A. (1998). Cation Migration and Coercivity in Mixed Copper-Cobalt Spinel Ferrite Powders. *Journal of Solid State Chemistry*, 141, pp. 56-63.